Double Broadband Balun Structure Using CRLH TL for Differential Excitation of Dual-Polarized Self-Grounded Bow-Tie Antenna

Sadegh Mansouri[1], John Kvarnstrand[2], Andrés Alayon Glazunov[1], Jian Yang[1], Per-Simon Kildal[1]

[1]Department of Signals and Systems, Chalmers University of Technology, Gothenburg, Sweden

[2]Bluetest AB, Gothenburg, Sweden

Abstract - A broadband compact balun comprising two composite right-left handed transmission lines (CRLH TL) is designed to excite a self-grounded bow-tie antenna. The design is based on a fractal shaped CRLH TL balun modified to the frequency band of interest. This balun consists of one +90° branch and three -90° branches to produce the desired 180° phase difference at the output. The simulated results show an amplitude imbalance of less than 1dB and a phase imbalance of less than 10°over most of the target bandwidth, i.e., 1.6-3 GHz. Two of the designed baluns were integrated with the bow-tie antenna in such a way that the feeding network could totally fit at the back of the antenna. The performance of the whole structure was also evaluated showing a return loss below -10 dB. The radiation pattern and the gain of the antenna with baluns are in good agreement with the ideal differential excitation, with gain degradation of only about 0.5dB in the worst case.

1. INTRODUCTION

It is well-known that the use of multiple port antennas at both the transmitter and the receiver sides of a communication link can improve the wireless communication system performance in terms of capacity and reliability for a given system bandwidth and transmitted power [1]. These so-called Multiple Input Multiple Output (MIMO) systems are at the core of 4G, 5G and the beyond wireless systems. In that respect, communication over orthogonally polarized wireless channels will be essential to achieve the anticipated performance. Therefore, designing antennas for base stations is of paramount significance to meet performance requirements. In 5G there is a particular interest in wideband micro-base stations that perform well both in rich isotropic multipath (RIMP) and in Random-Line-Of-Sight (RLOS) [2][3]. In addition, multi-port dual polarized wideband antennas can be used in many other applications. For example, in the Over-The-Air (OTA) testing of autonomous cars in a RLOS testing environment, a dual polarized uniform linear array antenna has been proposed as an essential part of the testing procedure [4]. One promising candidate for the array antenna element in such applications is the 4-port self-grounded bow-tie antenna [5]. This antenna can be used to provide a compact realization of a wideband dual-polarized antenna. However, in order to achieve the dual polarized performance by differentially exciting two ports of the bowtie antenna, we need to incorporate two baluns together with the antenna design. Each balun excites two opposite pedals of the bow-tie with a 180 degrees phase difference and 50Ω input impedance. So the antenna will produce two orthogonal polarizations. These baluns should satisfy the required bandwidth constraint (1.6-3GHz) and they also should have a compact structure in order to maintain a low profile. Despite the wideband characteristics of conventional microstrip baluns [6][7], they do not meet our compactness requirement. Furthermore, multilayer Marchand baluns [8] provide a very compact volume. On the other hand, they suffer from high manufacturing complexity and cost. Another option for the balun is the Composite Right Left Handed (CRLH) Transmission line (TL) which exploits the phase advance of the left handed materials [9][10][11]. In this paper, we employ the fractal shaped CRLH TL balun presented in [9] as a starting point of the design, but modify it to the frequency band of interest.

2. BALUN DESIGN PRECEDURE AND RESULTS

Fig. 1a) shows the phase variation with frequency of the 90° and the 270° transmission lines which are derived from the formula $\varphi = 2\pi d / \lambda$, where λ is the wavelength and d is the length of the

transmission line. Also, the frequency dependence of the phase for the LH and CRLH TL is shown in this figure. The LH and CRLH TL are designed to have a phase equal to 90° at the center frequency of 2GHz based on the following procedure. As we can see in this figure, a 270° TL is much more frequency dependent as compared to the 90° TL. Also, in practice, the physical length of the soldering pads of the elements results in having CRLH TL instead of a perfect LH TL. Thus, in order to meet the phase requirements, a CRLH TL is considered for both the 90° and the -90° branches.

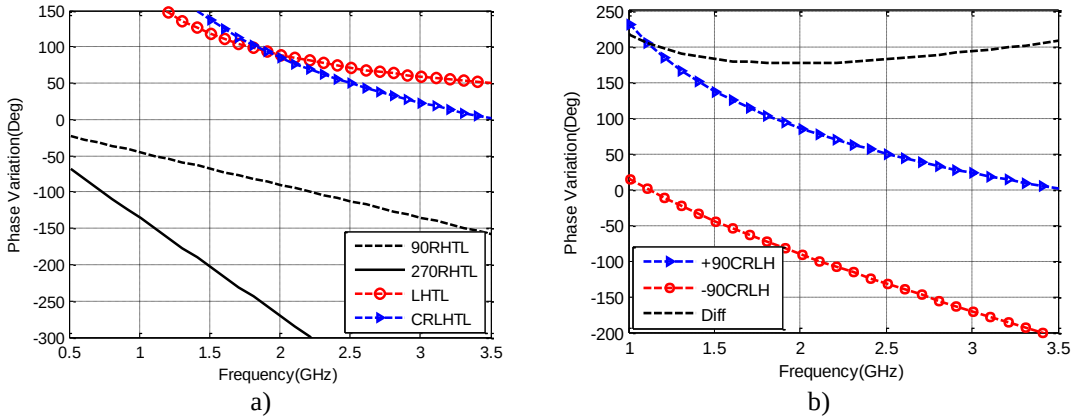

Fig. 1: Phase variation of a) 90° and 270° RHTL, LHTL and CRLHTL b) +90° CRLH and -90° CRLH and the difference

The schematic representation of the balun and the circuit model of each CRLH TL are shown in Fig 2 a) and b), respectively. As can be seen from Fig. 2, each TL comprises a right-handed part represented by capacitor C_R and inductor L_R as the electrical equivalent of the line itself and a left-handed part provided by the corresponding lumped elements. The balun has one 90° branch and three -90° branches.

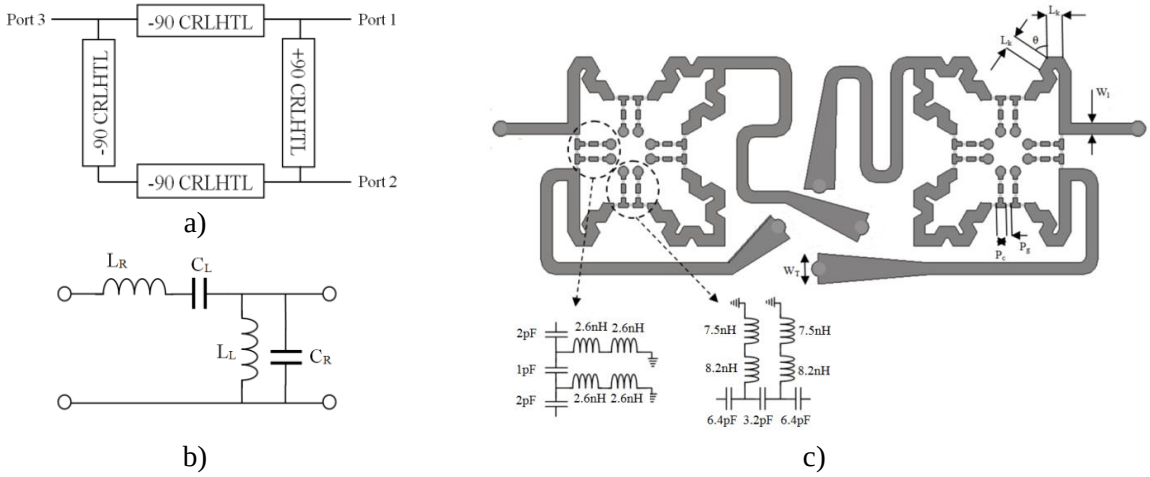

Fig. 2: a) Balun structure b) CRLH TL circuit model c) Dual balun geometry

Now, we present some conditions that are necessary to meet the phase and the amplitude requirements. First, the following condition should be satisfied for impedance matching [12]

$$Z_{C+} = \frac{Z_{C-}}{\sqrt{2}Z_{C-} - Z_0} Z_0, \qquad (1)$$

where Z_{C+} and Z_{C-} are the characteristic impedances of the +90° and -90° branches, respectively and Z_0 is the port impedance which is 50Ω. Further assuming that Z_{C+} and Z_{C-} are equal, we obtain from (1) that $Z_{C+} = Z_{C-} = \sqrt{2}Z_0$ .Secondly, we need to achieve the 180° phase difference between the output ports. The phase response of each branch can then be presented by

$$\varphi_{CRLHTL}(\omega) = -N\left(\omega\sqrt{L_R C_R} - \frac{1}{\omega\sqrt{L_L C_L}}\right), \quad (2)$$

where N is the number of CRLH cells in each branch and equals two in our case. Furthermore, in order to obtain the 180° phase difference over the required bandwidth, we set the first derivative of the phase difference respect to angular frequency equal to zero at 2 GHz. By enforcing this condition, a minimum would be appearing in $\varphi_{diff} = \varphi_{CRLHTL+} - \varphi_{CRLHTL-}$ at 2 GHz with a slow varying slope of phase difference around this frequency providing the phase requirements over the entire bandwidth (Fig. 1b). Using (1) and (2) together with the zero derivative condition, we can find the values of the elements of the CRLH cells in each branch. There are also some additional considerations for choosing these values. First, due to practical reasons, lumped elements should have commercially available values. Second, these values should not be large. This condition arises from the self-resonance frequency of the lumped elements above which the performance of the elements would change attributed to parasitic capacitance and inductance effects. Since elements with larger values have smaller resonance frequencies, they experience degradation in performance at higher frequencies. The third consideration is for the values which are equivalent to the length of the +90° branch. This length should be kept small and its minimum length will be determined, among other things, by the size of the soldering pads used in the +90° branch. After considering above mentioned criteria, the calculated values are shown in Table I. The phase response of the balun outputs and the difference between these two branches calculated by using derived values are shown in Fig 1b.

Table I: Calculated values of capacitors and inductors in CRLH circuit model of the +90° and the -90° branches

C_{L-}	L_{L-}	C_{R-}	L_{R-}	C_{L+}	L_{L+}	C_{R+}	L_{R+}
3.2pF	15.8nH	1.3pF	6.5nH	1pF	5nH	0.4pF	2nH

In this design, the fractal structure is used to achieve the desired compactness. A 36mm×100mm Rogers RO4003 with dielectric constant of 3.55 and thickness of 1.52mm is used as substrate. The initial dimensions of the fractal structure are based on the calculated values and formula in [13] and the electrical length of transmission line for the given values of C_R and L_R. Then by using CST Microwave Studio, a parametric study was performed to optimize the dimensions including length of the meandered TLs considering standard soldering pad sizes. For our application, we integrated two baluns with the bow-tie antenna in such a way that the dual balun could totally fit at the back of the antenna. Four transmission lines were added to the outputs of the balun to feed the bow-tie antenna pedals. In order to provide the same phase shift, they were chosen to have the same length. In addition, some tapering has been applied for impedance matching. The geometry of the balun is shown in Fig. 2c) with parameters given in Table II. The schematic circuit model for the lumped elements is detailed in Fig. 2c). The structure of the lumped element has been chosen in such a way to reduce the self-resonance effect of capacitors and inductors.

Table II: designed balun parameters

W_l	W_T	L_k	P_c	P_g	θ
2.55mm	4mm	2.15mm	1.35mm	0.6mm	30degrees

The S parameters of the designed dual balun are shown in Fig.3a). As illustrated, the amplitude of S_{11} is better than -10dB at 1.6-3GHz. Fig.3b) shows the amplitude and phase imbalance. The amplitude imbalance remains almost less than 1dB over most of the frequency band and the phase difference stays within ±10°.

3. BALUN INTEGRATION WITH THE BOW-TIE ANTENNA

The dual balun structure is integrated with the self-grounded bow-tie antenna as shown in Fig. 4a) and b). The dual balun completely fits into the area of the back side of the antenna with the four outputs connected to the each of the four pedals of the bow-tie. The reflection coefficients of the dual balun integrated with the bow-tie antenna and an ideal differentially excited bow-tie antenna are shown in Fig. 4c). To provide a more complete picture of the performance of the balun, the reflection

coefficients of the dual balun alone are also included in the figure. As can be seen, the return loss will remain below -10dB for most of the required bandwidth (1.67-3GHz).

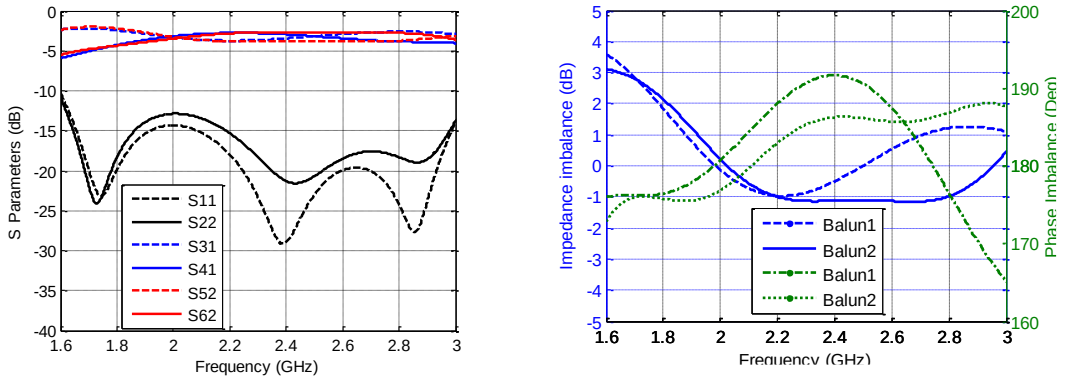

a) b)

Fig. 3: a) S parameters of baluns b) Impedance and phase imbalance of the outputs

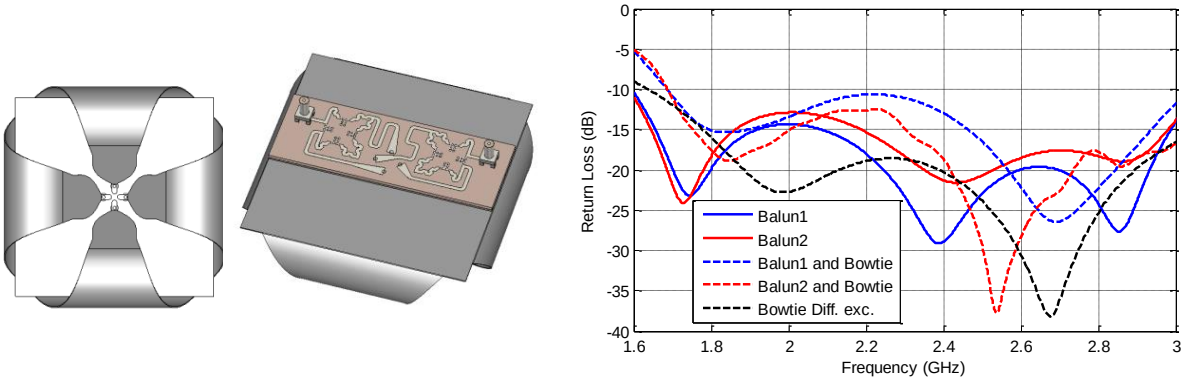

a) b) c)

Fig. 4: a) Self-grounded bow-tie antenna b) balun attached to the back of the bow-tie c) Return loss of the bow-tie antenna fed with balun, differentially excited bow-tie and each balun.

The radiation patterns of the bow-tie antenna integrated with the balun and the ideal excitation at the frequencies 1.6 GHz, 2.1 GHz and 3 GHz are shown in Fig. 5a), b) and c), respectively. The antenna gain as function of frequency is shown in Fig. 5d). As can be seen, using the dual balun reduces the antenna gain about 0.5 dB at most. The side-lobes levels increase up to 2.5 dB at the higher frequencies and the shape of the symmetry of the pattern will be only slightly perturbed due to the magnitude and phase imbalance of the balun.

4. CONCLUSION

A compact and broadband dual balun was design for differential excitation of a dual polarized bow-tie antenna. For the balun design, CRLH TLs were used to achieve the desired bandwidth and compactness characteristics. The reflection coefficient of the simulated balun was less than -10dB in the frequency band of 1.6-3GHz. The amplitude and the phase imbalances were approximately less than 1dB and 10°, respectively. In addition, the balun structure integrated with the self-grounded bow-tie antenna has shown very good simulated performance. For example, the radiation pattern of the whole structure was in good agreement with the ideal differentially excited bow-tie antenna with a gain reduction of only 0.5dB. The reflection coefficient remained below -10dB mostly over the entire bandwidth. Further work will include the verification of the design by measurements, as well as their evaluation in numerical and experimental Over-The-Air (OTA) setups.

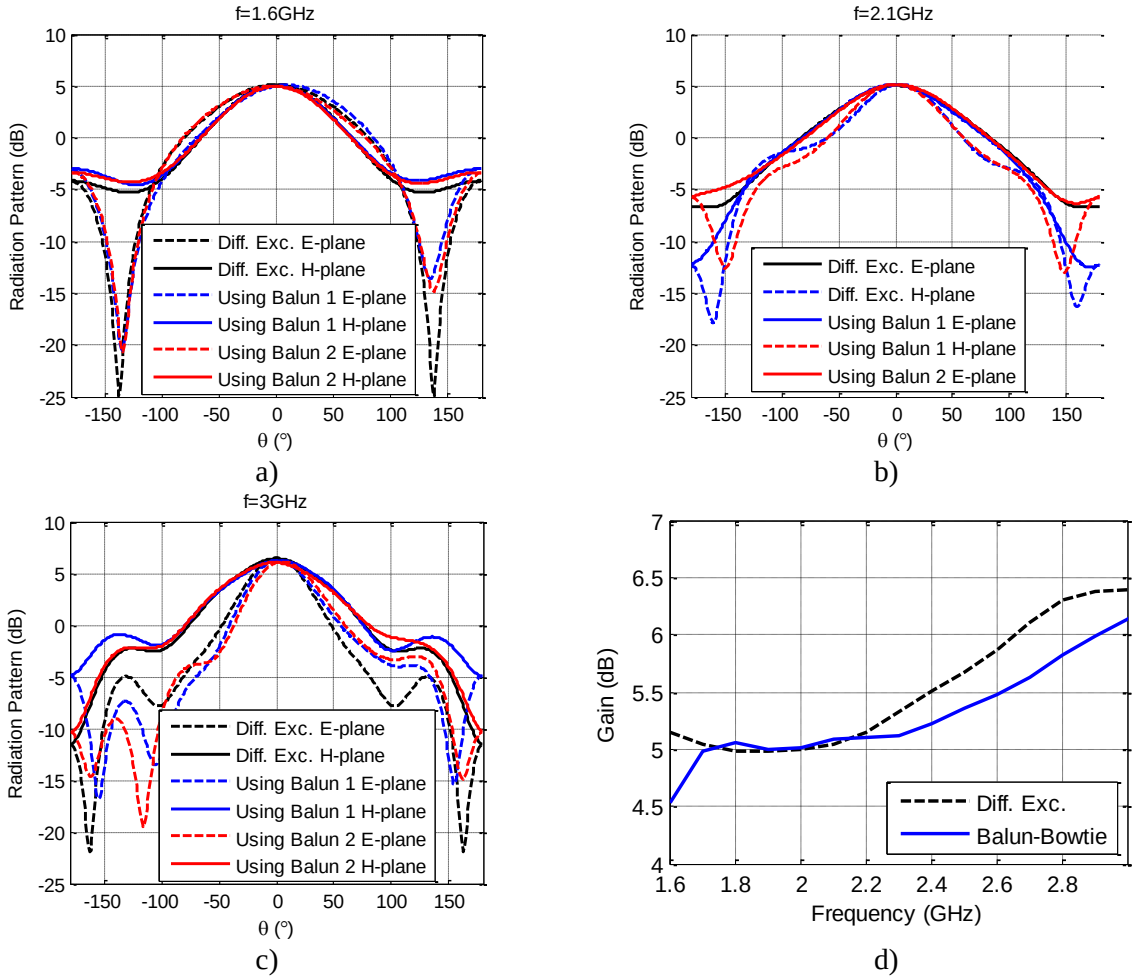

Fig. 5: Antenna radiation pattern at a) 1.6 GHz b) 2.1 GHz and c) 3 GHz and d) Gain of the bow-tie antenna with balun compared with the ideal differential excitation.

5. REFERENCES

[1] Molisch, A. F. (2010), Wireless Communications, 2nd ed., John Wiley, New York. ISBN: 978-0-470-74186-3.

[2] P.-S. Kildal, "Rethinking the Wireless Channel for OTA testing and Network Optimization by Including User Statistics: RIMP, pure-LOS, Throughput and Detection Probability," in ISAP 2013, Nanjing, China, Oct. 2013.

[3] P.-S. Kildal, X. Chen, M. Gustafsson, Z. Shen, "MIMO Characterization on System Level of 5G Micro Base Stations Subject to Randomness in LOS", IEEE Access, Vol. 22, pp. 1062-1075, Sept. 18, 2014.

[4] P.-S. Kildal, A. A. Glazunov, J. Carlsson, A. Majidzadeh, "Cost-effective measurement setups for testing wireless communication to vehicles in reverberation chambers and anechoic chambers," Antenna Measurements & Applications (CAMA), 2014 IEEE Conference on , pp.1,4, 16-19 Nov. 2014, doi: 10.1109/CAMA.2014.7003428.

[5] H. Raza, A. Hussain, J. Yang, and P.-S. Kildal, "Wideband compact 4-port dual polarized self-grounded bowtie antenna, " IEEE Trans. Antennas Propag., vol. 62, no. 9, pp. 4468_4473, Sep. 2014

[6] P. Wu, Z. Wang, and Y. Zhang, "Wideband planar balun using microstrip to CPW and microstrip to CPS transmissions," Electron. Lett., vol. 46, no. 24, pp. 1611-1613, Nov. 2010.

[7] Z. Y. Zhang, Y. X. Guo, L. C. Ong, and M. Y. W. Chia, "A new wide-band planar balun on a single-layer PCB," IEEE Microwave and Wireless Components Letters, vol. 15, no. 6, pp. 416–418, 2005.

[8] X. Lan, F. Fong, M. Kintis, K. Kono, D. Yamauchi, W. B. Luo, and D. Farkas, "An Ultra-Wideband Balun Using Multi-Metal GaAs MMIC Technology," IEEE Microw. Wireless Compon. Lett., vol. 20, pp. 474–476, Aug. 2010.

[9] Xu, H.-X., G.-M.Wang, X. Chen, and T.-P. Li, "Broadband balun using fully artificial fractal-shaped composite right/left-handed transmission line ," IEEE Microwave and Wireless Components Letters, Vol. 22, No. 1, 16-18, 2012.

[10] L. Fan, C. H. Ho, and K. Chang, "Wide-band reduced-size uniplanar magic-T, hybrid-ring, and de Ronde's CPW-slot couplers ," IEEE Trans. Microwave Theory Tech., vol. 43, pp. 2749–2758, Dec. 1995.

[11] H. Okabe, C. Caloz, and T. Itoh, "A compact enhanced-bandwidth hybrid ring using an artificial lumped-element left-handed transmission-line section," IEEE Trans. Microw. Theory Tech., vol. 52, no. 3, pp. 798–804, Mar. 2004.

[12] J.-L. Li, S.-W. Qu, and Q. Xue, "Miniaturised branch-line balun with bandwidth enhancement," *Electron. Lett.*, vol. 43, no. 17, pp. 931–932, Aug. 2007.

[13] I. Bahl, Lumped Elements for RF and Microwave Circuits. Boston, MA: Artech House, 2003, ch. 14, pp. 462–465.